

## Electron impact excitation of the $3d^{10}4p\ ^2P$ state in copper

M Ismail and P J O Teubner

School of Physical Sciences, The Flinders University of South Australia, GPO Box 2100, Adelaide, South Australia, 5001

Received 28 December 1994, in final form 31 May 1995

**Abstract.** Differential and total cross sections for the excitation of the  $3d^{10}4p\ ^2P$  state in copper by electrons have been measured at incident energies of 20, 40, 60, 80 and 100 eV. The differential cross sections cover the angular range from  $2.5^\circ$  to  $130^\circ$ . Absolute values of the cross sections have been assigned using a generalized oscillator strength technique and the validity of this technique is explored in some detail. The measured cross sections are compared with those predicted by several theories where it is found that the close-coupling calculation of Msezane and Henry accurately predicts the value of the total cross sections for incident energies greater than 20 eV. Agreement between theory and experiment for the differential cross sections is poor. The present measurements of the differential cross sections resolves the ambiguity in the absolute values of the cross sections measured by Trajmar and coworkers.

### 1. Introduction

Theories for the excitation of the  $3d^{10}4p\ ^2P$  state in copper have appeared in the literature for many years. One of the reasons for this interest is that excitation cross sections for this state are directly relevant to an understanding of the copper vapour laser. The first three states of the copper atom are the  $^2S$  ground state with configuration  $3d^{10}4s$ , the  $^2D$  state with configuration  $3s^24s^2$  and the  $^2P$  state with configuration  $3d^{10}4p$ . Excitation of the P state by electrons is favoured on angular momentum grounds over the D state excitation. Consequently a population inversion can be established between the P and D states and the system can be made to lase at 510.6 nm and 578.2 nm. A knowledge of the cross sections for the excitation of these states is clearly very relevant to an understanding of the copper vapour laser.

The first experiments on copper were reported by Williams and Trajmar (1974) who measured electron-impact differential cross sections for elastic scattering and for the excitation of the  $4^2P$  state at impact energies of 20 and 60 eV. These results were normalized to the Born integral elastic cross section. Subsequently Trajmar *et al* (1977) undertook a more extensive study of electron-impact cross sections for elastic scattering and for the excitation of the  $4^2P$  and  $3^2D$  states at incident energies of 6, 10, 20, 60 and 100 eV in the angular range from  $15^\circ$  to  $140^\circ$ . In this case they normalized their relative angular distributions using helium as a secondary standard and by normalizing the data to the static exchange calculation of Winter (1977) for elastic scattering at 100 and  $40^\circ$ . This work yielded integral cross sections which were about a factor of two less than those reported in the previous work but they noted no justification of the suggested factor of seven reduction in cross sections which had been reported by Trainor *et al* (1975).

Aleksakhin *et al* (1979) and Borozdin *et al* (1977) have reported integral cross section measurements for the excitation of the  $4^2P$  state in the energy range from 10 to 75 eV.

Both groups used a crossed-beam technique. The cross sections reported by Aleksakhin *et al* (1979) were less than the values of Trajmar *et al* (1977).

Recently Flynn *et al* (1993) have reported measurements of integral cross sections for the measurement of the excitation of the  $4^2\text{P}$  state from threshold (3.8 eV) up to 8 eV. These results were taken by observing the 324 and 327 nm photons arising from the decay of the  $4^2\text{P}$  state. Estimates were made of the contribution of cascades to the observed signal and the excitation function was normalized to the Born cross section at 1000 eV.

Msezane and Henry (1986a, b) have used a close-coupling approximation to study the excitation of the  $4^2\text{P}$  state, the  $3^2\text{D}$  and  $4^2\text{D}$  states in the energy range between 6 and 100 eV. Four states were included in this calculation and sophisticated target wavefunctions were used. Previously (Msezane and Henry 1985) these authors had investigated the normalization of the Trajmar *et al* (1977) results. They used a generalized oscillator strength formalism and deduced that an energy-independent normalizing factor of 0.36 should be applied to the experimental data. Favourable agreement with the experimental integral cross sections was obtained with this approach for incident energies  $\geq 60$  eV. Msezane and Henry (1986a) proposed that further experiments should be carried out so that the discrepancy between theory and experiment could be resolved.

Scheibner *et al* (1987) have used a four-state close-coupling calculation to describe scattering of electrons from copper from threshold to 8 eV. This calculation has been extended by including up to 10 states in the expansion by Scheibner and Hazi (1993). Excellent agreement was found when these calculations were compared with the measured integral cross sections of Flynn *et al* (1993).

Using a distorted-wave approach, Pangantiwar and Srivastava (1988) studied the excitation of the  $3\text{d}^{10}4\text{p } ^2\text{P}$  state by electron impact in the energy range from threshold to 100 eV. Exchange is included and a simple form of the polarization potential is used in one series of calculations. They compare their results with the renormalized results of Trajmar *et al* (1977) as proposed by Msezane and Henry (1986a, b). The agreement with the integral cross sections between the 'experiment' and theory is poor as is the agreement between theory and the differential cross sections. These authors suggest the need for further measurements.

The several Born approximation calculations which have been reported are those by Winter (1977), Peterkop and Liepinsh (1979) and by Pangantiwar and Srivastava (1988). All calculations disagree with each other and with the renormalized experimental integral cross section. Msezane and Henry (1986a) attribute the failure of these calculations to inadequacies in the wavefunctions which were used. In the present context the absence of an appropriate Born calculation presented significant difficulties to normalizing our relative angular distributions to differential cross sections. These difficulties were addressed by using a generalized oscillator strength (GOS) approach. This technique was first employed by Lassette's group (Lassette *et al* 1969) to normalize cross sections for electron scattering from helium but it has been used subsequently by several groups in the scattering of electrons from metal vapours; for example, Williams and Trajmar (1977) in potassium, Shuttleworth *et al* (1979) in lithium and Brunger *et al* (1988) in magnesium. Trajmar *et al* (1977) explored its use in their work in copper but abandoned the technique because of small signal levels in the inelastic channel at 100 eV. The technique depends on the fact that the generalized oscillator strengths tend to the optical oscillator strength as  $K^2 \rightarrow 0$  where  $K$  is the momentum transfer. Its use also depends on the validity of the relationship between the GOS and the differential cross section; that is on the validity of the first Born approximation.

The experimental techniques used in the present study are described in section 2 together with a quantitative discussion of the use of the GOS to normalize the cross sections. The results are presented and discussed in section 3 and the conclusions are given in section 4.

## 2. Experimental techniques

The experiments were conducted in a modulated crossed-beam apparatus which has been described in detail by Teubner *et al* (1986). A beam of copper atoms was produced in a molybdenum oven which was heated to 1600 K by electron bombardment. After emerging from a 1 mm aperture in the oven, the copper beam was collimated and chopped by a rotating toothed wheel. After further collimation the modulated beam entered the interaction region where it intersected with a well focused electron beam. The diameter of the copper beam in the interaction region was observed to be 3.5 mm.

The energy of the electrons which had been scattered from the interaction region through an angle  $\theta$  was analysed by a cylindrical mirror electron spectrometer which was set to pass electrons which had excited the  $4^2P$  state and had therefore lost 3.8 eV of their energy. The overall energy resolution of the electron beam and spectrometer was 0.8 eV which was sufficient to resolve not only those electrons which had excited the  $3^2D$  state but also those from higher states. A typical energy loss spectrum is shown in figure 1.

After analysis the electrons were detected by a channel electron multiplier pulse from which they were amplified and counted in either of two gated counters. The counters were enabled by a reference signal which was derived from the chopper which modulated the copper beam. The phase of the reference signal was adjusted so that one counter recorded events when the copper beam was in the interaction region. These counts were proportional to the number of electrons scattered from the beam and the background. The other recorded events when the beam was off; these counts were proportional to scattering from the background. The difference between the counts in the two counters was proportional to the number of electrons scattered from the copper beam at a particular angle,  $I(\theta)$ . This procedure was followed at a series of angles  $\theta$  by rotating the spectrometer about an axis defined by the atomic beam.

Care was taken to identify and eliminate possible sources of systematic error in the present measurements. Electric fields were eliminated from the interaction region by shielding all potential sources such as the gun, feedthroughs, leads and the electron spectrometer. The ambient magnetic field was minimized by enclosing the scattering chamber with three sets of Helmholtz coils and lining the apparatus with mu-metal shielding. The magnetic field in the interaction region was measured to be less than 5 mgauss.

It was found that the temperature of the molybdenum crucible, which was monitored

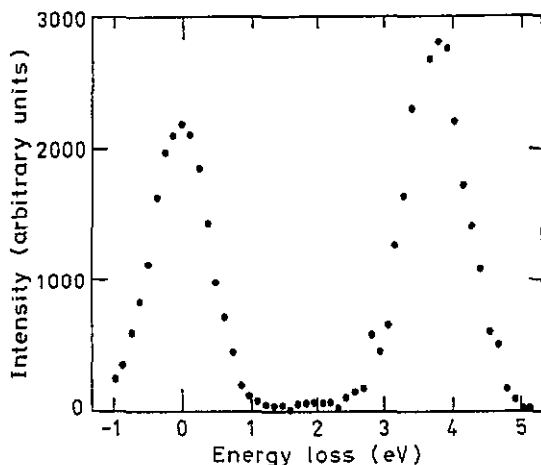


Figure 1. A typical energy loss spectrum  $E_0 = 60$  eV,  $\theta = 15^\circ$  showing the elastic peak and the peak corresponding to the excitation of the  $3d^{10}4p\ ^2P$  state of Cu.

throughout the experiments, varied by  $\pm 2$  K over the course of each run. This temperature variation resulted in a  $\pm 3\%$  change in the density of copper atoms in the beam and consequently to the scattered signal from the copper beam which was observed. The scattered intensity was corrected to account for this effect. The incident electron beam current was monitored in a Faraday cup throughout the experiments and it was found to be constant to within 1%. The dynamic range of the scattered electron signal was very large. The signal at the higher energies changed by five orders of magnitude over the angular range from  $3^\circ$  to  $130^\circ$ . Although we established that the scattered electron detector response was linear up to 40 kHz, care was taken to ensure that the scattered electron count rate did not exceed 20 kHz at forward angles. Thus we were forced to take three sets of angular distributions from  $\theta_{min}$  to  $25^\circ$ ,  $12^\circ$  to  $60^\circ$  and  $40^\circ$  to  $130^\circ$ . The final angular distribution at each energy was formed from a composite of each run.

The zero in the scattering angle was determined by taking angular distributions for both positive and negative scattering angles and by requiring that the distributions were symmetric about  $0^\circ$ . A further check on the zero was provided by sweeping the electron spectrometer through the electron beam. It was found that the zero deduced from both techniques agreed to within  $\pm 0.2^\circ$ .

The field of view of the electron spectrometer was much greater than the diameter of the copper beam. Thus all of the interaction region was viewed by the spectrometer at all scattering angles.

The angular distribution of electrons scattered from the beam was

$$I(\theta) = \frac{I_0}{e} n_a \ell d\Omega \eta \tau \sigma(\theta) \quad (1)$$

where  $I_0$  was the incident electron beam current,  $e$  the electronic charge,  $n_a$  the density of copper atoms in the beam,  $\ell d\Omega$  the effective solid angle,  $\eta$  the efficiency,  $\tau$  the transmission and  $\sigma(\theta)$  the differential cross section.

An absolute measurement of  $\sigma(\theta)$  requires the absolute measurement of each of the factors in (1). This is known to be extremely difficult to do in a crossed-beam configuration. Therefore a different approach was followed in these experiments.

At each incident electron beam energy an experimental procedure was chosen so that parameters such as  $I_0$ ,  $n_a$ ,  $\ell d\Omega$ ,  $\eta$  and  $\tau$  are constant. Thus equation (1) can be written as

$$I(\theta) = C \sigma(\theta) \quad (2)$$

where

$$C = \frac{I_0}{e} n_a \ell d\Omega \eta \tau. \quad (3)$$

A knowledge of the differential cross section at one angle then determines the constant  $C$  for that incident energy. In the present case we have determined  $C$  by using the concept of the generalized oscillator strength (GOS).

In terms of the GOS,  $f(K)$ , the relationship with the differential cross section is given (in atomic units) by (Mott and Massey 1965)

$$\sigma(\theta) = \frac{2}{W} \frac{k_n}{k_0} \frac{f(K)}{K^2} \quad (4)$$

where  $W$  is the binding energy of the excited state and  $K$  is the momentum transfer between the incident momentum  $k_0$  and the final momentum  $k_n$  of the electron scattered through an angle  $\theta$ .

That is

$$K = k_0 - k_n. \quad (5)$$

It can be shown that for small  $K^2$  (Brunger *et al* 1988)

$$f(K) = f_0 - AK^2 + BK^4. \quad (6)$$

The GOS technique involves the determination of  $f(K)$  from (6). Equation (4) can then be used to determine  $\sigma(\theta)$  at one angle, hence  $C$  and the differential cross section at all angles.

In particular,

$$I(\theta) = \frac{2C k_n}{W k_0} \frac{f(K)}{K^2}. \quad (7)$$

The usual approach, e.g. Trajmar *et al* (1977), Buckman and Teubner (1979), is to determine a relative GOS from (7) by forming the product  $IK^2$

$$\begin{aligned} IK^2 &= f_{\text{rel}}(K) \\ &= C' f(K) \end{aligned} \quad (8)$$

where

$$C' = \frac{2C k_n}{W k_0}. \quad (9)$$

Equation (6) implies that for small  $K^2$ ,  $f(K)$  will be a monotonically decreasing function of  $K^2$  and that  $f_0$  is approached from below as  $K^2 \rightarrow 0$ . The data of Trajmar *et al* (1977) for the excitation of the  $4^2P$  state in copper, however, implies that the GOS approaches  $f_0$  from above. A qualitative explanation of this behaviour has been given by Msezane and Henry (1985) who speculate that turning points in the function  $IK^2$  could arise because of the relative variation in the quantities  $I(K)$  and  $K^2$  near  $\theta = 0$ . Turning points could, however, also indicate sources of systematic error; for example if the constant  $C'$  depended on the scattering angle at small angles. Another possible source of the turning point could be saturation in the electron detector.

Figure 2 shows a plot of  $IK^2$  versus  $K^2$  at an incident electron energy of 60 eV. The turning point in the GOS at  $K^2 = 0.021$  is clearly identified. This corresponds to a scattering angle of  $3.6^\circ$ . In this case the count rate at the detector was less than 1 kHz so the data were independent of saturation effects. The apparatus was also carefully aligned so that the electron spectrometer accurately rotated about an axis formed by the copper beam. Consequently another explanation of the phenomenon was sought.

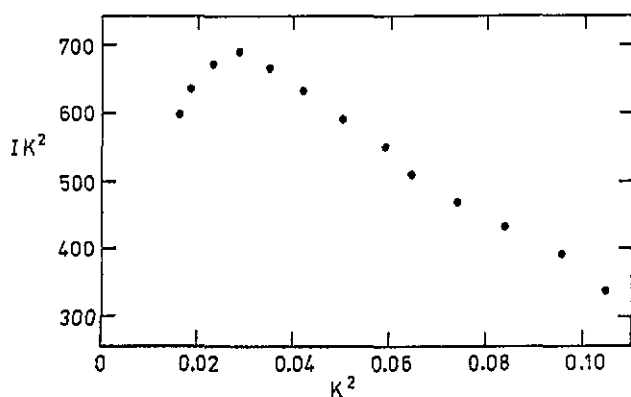


Figure 2. The product  $IK^2$  at an incident energy of 60 eV for small values of  $K^2$ .

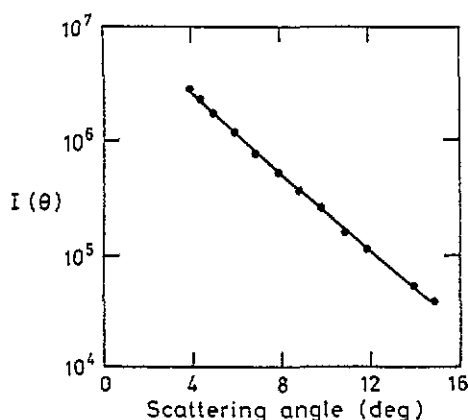


Figure 3. The angular distribution  $I(\theta)$  for inelastic scattering at an incident energy of 60 eV at small scattering angles.

Figure 3 shows a plot of the angular distribution of inelastically scattered electrons from the  $4^2P$  state in copper at an incident electron energy of 60 eV at small angles  $\theta$ . Clearly the angular distribution can be represented by

$$I(\theta) = I_0 \times 10^{-b\theta} \quad (10)$$

$$= I_0 e^{-\beta\theta} \quad (11)$$

where

$$\beta = b \ln 10.$$

For small  $K^2$  the momentum transfer in atomic units is given by

$$K^2 = 2E_0 \left[ \left( \frac{W}{2E_0} \right)^2 + \theta^2 \right] \quad (12)$$

where  $E_0$  is the incident energy.

Thus

$$IK^2 = 2E_0 I_0 e^{-\beta\theta} \left[ \left( \frac{W}{2E_0} \right)^2 + \theta^2 \right] \quad (13)$$

which has turning points at angles  $\theta$  such that

$$\theta = \left[ \frac{1 \pm \sqrt{1 - \left( \frac{\beta W}{2E_0} \right)^2}}{\beta} \right]. \quad (14)$$

At 60 eV,  $\beta = 24.9$ ,  $W = 0.14$  au and turning points are expected at  $1^\circ$  and  $3.6^\circ$ . The latter turning point is confirmed by the data in figure 2.

Consequently a fit to the function  $IK^2$  of the form of (6) may lead to errors in the derived values of  $A$  and  $B$  unless the regions around the turning points are excluded. On the other hand (7) can be viewed as

$$I(K) = C' f(K)/K^2. \quad (15)$$

That is

$$I(K) = \frac{C' f_0}{K^2} - C'A + BC'K^2 \quad (16)$$

$$= \frac{D}{K^2} - E + GK^2. \quad (17)$$

Angular distributions were fitted using (16) at each energy. The coefficients  $D$ ,  $E$  and  $G$  were found from the fit at each energy. Specifically

$$C' = \frac{f_0}{D} \quad (18)$$

$$A = \frac{E}{C'} \quad (19)$$

$$B = \frac{G}{C'}. \quad (20)$$

The optical oscillator strength  $f_0 = 0.645$  (Hannaford and MacDonald 1978).

The value of  $C'$ , determined from (17) and (18) is sufficient to normalize the value of the cross section from (9) and (2). Equations (19) and (20) can be used to evaluate the GOS at each energy. It was found that for small  $K^2$ ,

$$f(K) = 0.645 - 4.8K^2 + 21.2K^4. \quad (21)$$

The GOS concept is based on the first Born approximation and the use of the technique depends heavily on the validity of this approximation in the energy range under consideration. It is clear from (21) that  $f(K)$  only depends on the momentum transfer and not on the incident energy. Thus a necessary condition for the validity of the GOS formalism is that the experimental data should satisfy (21) at each energy. Figure 4 shows the derived generalized oscillator strengths as a function of  $K^2$ . In view of the ambiguities in turning points discussed above, data near the turning points have been omitted. The derived GOS are independent of the incident energy to within experimental error.

### Integral cross sections

Integral cross sections  $Q$  for the excitation of the  $3d^{10}4p\ ^2P$  state were derived by integrating the differential cross sections over the scattering angle using Simpson's rule. That is

$$Q = 2\pi \int_0^{2\pi} \sigma(\theta) \sin \theta d\theta.$$

The differential cross sections at all the energies studied in the present experiments were very strongly peaked in the forward direction. At 20 eV 84% of the integral came from the angular range less than  $15^\circ$  whilst at 100 eV 99% of the integral came from the range 0 to  $14^\circ$ .

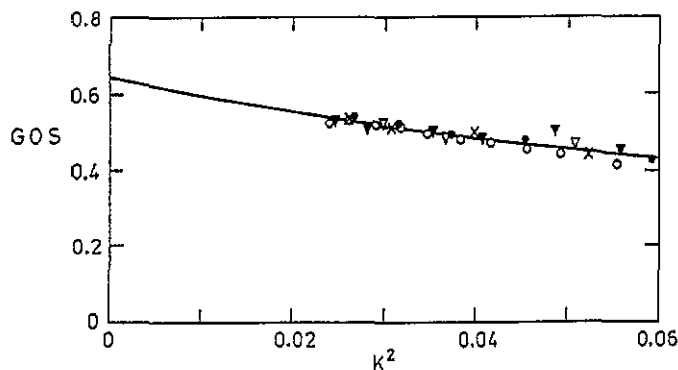


Figure 4. Experimentally derived generalized oscillator strengths at incident energies of (○) 20 eV; (●) 40 eV; (▽) 60 eV; (▽) 80 eV; (×) 100 eV. The curve is given by (21) in the text.

Equation (21) was used to extrapolate the measured data to  $0^\circ$ . In each case this extrapolation covered a small but significant angular range. For example at 100 eV the range was extended from the measurements at  $2.2^\circ$  whilst at 20 eV the last measurement was taken at  $5^\circ$ .

### 3. Results and discussion

#### *Integral cross sections*

The integral cross sections for the excitation of the  $3d^{10}4p\ ^2P$  state are given in table 1 and are displayed in figure 5. They are compared with the predictions of several theories and with previous measurements. The error bars represent one standard deviation variation in the several sets of results which were taken at each energy. It is clear that there is excellent agreement between the present data and the predictions of the coupled channels theory of Msezane and Henry (1986a) for energies greater than 20 eV. Trajmar *et al* (1977) determined the integral cross section by integrating their differential cross sections in the same manner as has been described above. However, they made no measurements below  $15^\circ$  and the results were extrapolated to zero degrees. At 60 eV the angular range greater than  $15^\circ$  contributes about 1% to the integral cross section. Thus their integral cross section at 60 eV reflects both the validity of the theory used to normalize the data and that of the extrapolation procedure. Given these uncertainties it is not surprising that there is poor agreement between the present results at 60 eV and that of Trajmar *et al* (1977). Although the differential cross

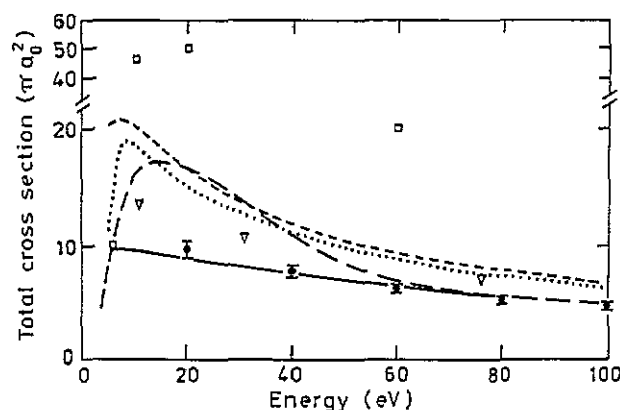


Figure 5. Total cross sections for the excitation of the  $3d^{10}4p\ ^2P$  state in copper. The present results ( $\bullet$ ) are compared with the measurements of Trajmar *et al* (1977) ( $\square$ ), and Aleksakhin *et al* ( $\nabla$ ) and with the predictions of the four-state close-coupling calculation of Msezane and Henry (1986a) (—), the impact parameter calculation of Winter and Hazi (1982) (---) and with the distorted-wave calculations of Pangantiwar and Srivastava (1988) (- - -) (DWPE) and (.....) (DWΞ).

Table 1. Integral cross sections for the excitation of the  $3d^{10}4p\ ^2P$  state in copper. The units are  $\pi a_0^2$  and the errors represent plus and minus one standard deviation.

E (eV)	20	40	60	80	100
$Q(\pi a_0^2)$	$9.74 \pm 0.71$	$7.73 \pm 0.52$	$6.20 \pm 0.42$	$5.20 \pm 0.36$	$4.60 \pm 0.35$



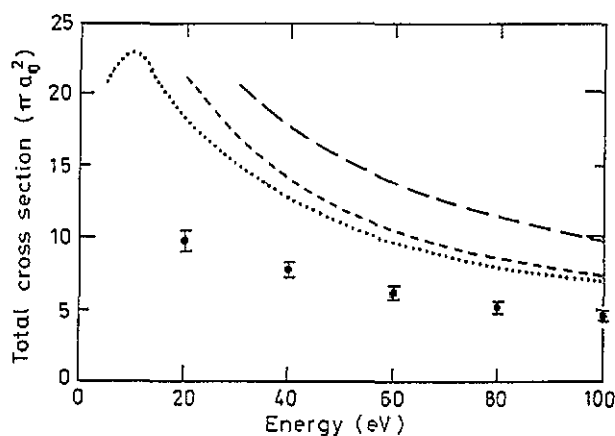


Figure 6. Total cross sections for the excitation of the  $3d^{10}4p^2P$  state in copper. The present results (•) are compared with the predictions of the first Born approximation calculations of Pangantiwar and Srivastava (1988) (.....), Winter (1977) (— — —), Peterkop and Liepinsh (1979) (— · —).

sections are not so strongly forward peaked at 20 eV, similar arguments apply.

The present results do not support the previous results of Aleksakhin *et al* (1979) which are clearly too large.

Three Born approximation calculations are shown in figure 6; that by Winter (1977), by Peterkop and Liepinsh (1979) and by Pangantiwar and Srivastava (1988). All differ from each other and from the present results. Msezane and Henry (1986a) attributed the difference between the first two calculations to the different descriptions of the target wavefunctions used in the theories. For example, the wavefunction used by Winter gave 1.257 for the optical oscillator strength whilst that used by Peterkop and Liepinsh (1979) gave 0.92. The oscillator strength derived from the wavefunctions used by Pangantiwar and Srivastava (1988) is not quoted, however, generalized oscillator strengths can be computed from their differential cross sections and extrapolated to zero momentum transfer using the techniques outlined above. We find that the optical oscillator strength indicated from this procedure is  $f_0 = 1$ .

Msezane and Henry (1986b) assert that Born calculations based on the wavefunctions used in their calculations which give an oscillator strength of 0.64 would give lower cross sections than those of Peterkop and Liepinsh. They imply that these Born calculations would agree with their close-coupling results at energies greater than 50 eV.

The procedure which has been used to normalize the present experimental results implies that the cross sections should agree with those predicted by the Born approximation at a sufficiently high impact energy. That they obviously do not agree with the Born calculations shown in figure 6 can be attributed to inadequacies in the wavefunctions used in the calculations. The semiclassical impact parameter calculations of Winter and Hazi (1982) which used appropriate wavefunctions agree with the present results at energies greater than 60 eV.

The total cross sections predicted by Pangantiwar and Srivastava using a distorted-wave theory with exchange do not agree with the present results. However, the discussion above indicates that the problem may lie in the description of the bound states rather than the scattering theory.

*Differential cross sections*

The present differential cross sections for the excitation of the  $3d^{10}4p\ ^2P$  state in copper are given in tables 2 and 3 for incident electron energies of 20, 40, 60, 80 and 100 eV. The errors are statistical in origin and represent plus and minus one standard deviation of the mean. The present data at 20 eV are shown in figure 7. We compare our results with those of Trajmar *et al* (1977). There is clearly a large difference between the absolute values of the two sets of measurements that cannot be accounted for by the error limit of a factor of about two in the absolute value cited in the earlier work. We have normalized the two sets of measurements at  $80^\circ$  so that the shapes of the two angular distributions can be compared. There is good agreement in shape between the two sets except at backward angles where the differences cannot be explained by the relative error in the two sets of measurements. The minimum in the angular distributions at about  $80^\circ$  is not predicted by either theory.

**Table 2.** Differential cross sections for the excitation of the  $3d^{10}4p\ ^2P$  state in copper at incident electron energies of 20 and 40 eV. The units are  $a_0^2$  per steradian. The errors represent one standard deviation and are statistical in origin.

$\theta$ (deg.)	20 eV	40 eV
4	—	$3.60E(2) \pm 7.02E(0)$
5	$2.73E(2) \pm 5.10E(0)$	$2.53E(2) \pm 3.09E(0)$
6	$2.29E(2) \pm 4.21E(0)$	$1.77E(2) \pm 2.20E(0)$
7	$1.88E(2) \pm 3.81E(0)$	$1.27E(2) \pm 2.00E(0)$
8	$1.51E(2) \pm 2.20E(0)$	$9.02E(1) \pm 1.72E(0)$
9	$1.23E(2) \pm 2.10E(0)$	$6.49E(1) \pm 1.48E(0)$
10	$9.8E(1) \pm 1.99E(0)$	$4.85E(1) \pm 9.12E(-1)$
12	$5.35E(1) \pm 1.13E(0)$	$2.60E(1) \pm 4.01E(-1)$
14	$3.29E(1) \pm 5.32E(-1)$	$1.35E(1) \pm 1.09E(-1)$
16	$1.99E(1) \pm 3.61E(-1)$	$7.73E(0) \pm 1.36E(-1)$
18	$1.17E(1) \pm 2.42E(-1)$	$4.27E(0) \pm 3.93E(-2)$
20	$8.41E(0) \pm 8.51E(-2)$	$2.56E(0) \pm 4.07E(-2)$
25	$3.19E(0) \pm 6.38E(-2)$	$7.04E(-1) \pm 1.68E(-2)$
30	$1.41E(0) \pm 4.22E(-2)$	$2.90E(-1) \pm 7.45E(-3)$
35	$7.01E(-1) \pm 2.80E(-2)$	$1.48E(-1) \pm 5.15E(-3)$
40	$3.51E(-1) \pm 2.11E(-2)$	$6.97E(-2) \pm 2.39E(-3)$
45	$2.42E(-1) \pm 1.69E(-2)$	$3.61E(-2) \pm 2.32E(-3)$
50	$1.32E(-1) \pm 1.06E(-2)$	$1.94E(-2) \pm 1.81E(-3)$
55	$7.37E(-2) \pm 5.89E(-3)$	$1.68E(-2) \pm 1.8E(-3)$
60	$3.82E(-2) \pm 3.44E(-3)$	$1.89E(-2) \pm 9.60E(-4)$
65	—	—
70	$1.31E(-2) \pm 1.15E(-3)$	$2.14E(-2) \pm 1.08E(-3)$
75	—	—
80	$9.17E(-3) \pm 1.38E(-3)$	$1.52E(-2) \pm 1.02E(-3)$
85	—	—
90	$7.44E(-3) \pm 1.49E(-3)$	$9.28E(-3) \pm 7.94E(-4)$
95	—	—
100	$1.12E(-2) \pm 1.57E(-3)$	$6.09E(-3) \pm 6.47E(-4)$
105	—	—
110	$1.31E(-2) \pm 1.71E(-3)$	$5.41E(-3) \pm 8.05E(-4)$
115	—	—
120	$1.86E(-2) \pm 1.87E(-3)$	$5.50E(-3) \pm 1.04E(-3)$
125	—	—
130	$3.96E(-2) \pm 3.02E(-3)$	—

Table 3. As for table 2 except at incident energies of 60, 80 and 100 eV.

$\theta$ (deg.)	60 eV	80 eV	100 eV
2.2	$7.10\text{E}(2) \pm 1\text{E}(1)$	—	5.48
2.5	$6.16\text{E}(2) \pm 8.8\text{E}(0)$	$5.6\text{E}(2) \pm 7.1\text{E}(0)$	$4.63\text{E}(2) \pm 6.3\text{E}(0)$
3	$4.76\text{E}(2) \pm 6.8\text{E}(0)$	$4.31\text{E}(2) \pm 5.5\text{E}(0)$	$3.36\text{E}(2) \pm 4.6\text{E}(0)$
3.5	$3.63\text{E}(2) \pm 5.2\text{E}(0)$	$3.08\text{E}(2) \pm 3.9\text{E}(0)$	$2.50\text{E}(2) \pm 3.4\text{E}(0)$
4	$2.87\text{E}(2) \pm 4.09\text{E}(0)$	$2.35\text{E}(2) \pm 2.99\text{E}(0)$	$1.84\text{E}(2) \pm 2.5\text{E}(0)$
5	$1.82\text{E}(2) \pm 3.10\text{E}(0)$	$1.53\text{E}(2) \pm 2.00\text{E}(0)$	$1.15\text{E}(2) \pm 1.00\text{E}(0)$
6	$1.27\text{E}(2) \pm 2.22\text{E}(0)$	$8.90\text{E}(1) \pm 1.70\text{E}(0)$	$7.23\text{E}(1) \pm 9.1\text{E}(-1)$
7	$8.13\text{E}(1) \pm 2.01\text{E}(0)$	$5.42\text{E}(1) \pm 4.74\text{E}(-1)$	$4.32\text{E}(1) \pm 5.38\text{E}(-1)$
8	$5.79\text{E}(1) \pm 1.30\text{E}(0)$	$3.15\text{E}(1) \pm 3.15\text{E}(-1)$	$3.00\text{E}(1) \pm 3.60\text{E}(-1)$
9	$3.88\text{E}(1) \pm 8.04\text{E}(-1)$	$2.09\text{E}(1) \pm 2.09\text{E}(-1)$	$1.93\text{E}(1) \pm 2.32\text{E}(-1)$
10	$2.71\text{E}(1) \pm 2.61\text{E}(-1)$	$1.38\text{E}(1) \pm 1.98\text{E}(-1)$	$1.15\text{E}(1) \pm 1.74\text{E}(-1)$
12	$1.23\text{E}(1) \pm 1.36\text{E}(-1)$	$5.96\text{E}(0) \pm 7.88\text{E}(-2)$	$4.69\text{E}(0) \pm 9.38\text{E}(-2)$
14	$6.32\text{E}(0) \pm 1.36\text{E}(-1)$	$2.81\text{E}(0) \pm 5.15\text{E}(-2)$	$1.96\text{E}(0) \pm 5.72\text{E}(-2)$
16	$3.13\text{E}(0) \pm 6.46\text{E}(-2)$	$1.31\text{E}(0) \pm 2.20\text{E}(-2)$	$8.43\text{E}(-1) \pm 3.81\text{E}(-2)$
18	$1.46\text{E}(0) \pm 2.98\text{E}(-2)$	$6.10\text{E}(-1) \pm 1.56\text{E}(-2)$	$3.61\text{E}(-1) \pm 2.75\text{E}(-2)$
20	$7.36\text{E}(-1) \pm 2.21\text{E}(-2)$	$3.13\text{E}(-1) \pm 9.92\text{E}(-3)$	$2.07\text{E}(-1) \pm 1.90\text{E}(-2)$
25	$2.21\text{E}(-1) \pm 2.98\text{E}(-3)$	$1.36\text{E}(-1) \pm 4.14\text{E}(-3)$	$8.57\text{E}(-2) \pm 1.03\text{E}(-2)$
30	$8.99\text{E}(-2) \pm 2.62\text{E}(-3)$	$5.14\text{E}(-2) \pm 2.57\text{E}(-3)$	$4.40\text{E}(-2) \pm 6.16\text{E}(-3)$
35	$4.44\text{E}(-2) \pm 1.74\text{E}(-3)$	—	$2.50\text{E}(-2) \pm 6.73\text{E}(-3)$
40	$2.07\text{E}(-2) \pm 2.20\text{E}(-3)$	$1.58\text{E}(-2) \pm 1.45\text{E}(-3)$	$1.63\text{E}(-2) \pm 2.91\text{E}(-3)$
45	$1.19\text{E}(-2) \pm 1.25\text{E}(-3)$	$1.53\text{E}(-2) \pm 1.90\text{E}(-3)$	$1.74\text{E}(-2) \pm 2.35\text{E}(-3)$
50	$1.28\text{E}(-2) \pm 1.21\text{E}(-3)$	$1.66\text{E}(-2) \pm 2.29\text{E}(-3)$	$1.76\text{E}(-2) \pm 2.36\text{E}(-3)$
55	$1.23\text{E}(-2) \pm 6.16\text{E}(-4)$	$1.74\text{E}(-2) \pm 1.99\text{E}(-3)$	$1.83\text{E}(-2) \pm 2.82\text{E}(-3)$
60	$1.31\text{E}(-2) \pm 6.55\text{E}(-4)$	$1.64\text{E}(-2) \pm 1.74\text{E}(-3)$	$1.51\text{E}(-2) \pm 2.93\text{E}(-3)$
65	$1.39\text{E}(-2) \pm 6.94\text{E}(-4)$	$1.45\text{E}(-2) \pm 1.81\text{E}(-3)$	$1.06\text{E}(-2) \pm 2.42\text{E}(-3)$
70	$1.22\text{E}(-2) \pm 7.32\text{E}(-4)$	$1.13\text{E}(-2) \pm 1.68\text{E}(-3)$	$8.58\text{E}(-3) \pm 1.87\text{E}(-3)$
75	$8.40\text{E}(-3) \pm 6.66\text{E}(-4)$	$7.56\text{E}(-3) \pm 1.35\text{E}(-3)$	$5.49\text{E}(-3) \pm 1.72\text{E}(-3)$
80	$5.71\text{E}(-3) \pm 5.09\text{E}(-4)$	$6.2\text{E}(-3) \pm 1.26\text{E}(-3)$	$5.38\text{E}(-3) \pm 1.32\text{E}(-3)$
85	$5.08\text{E}(-3) \pm 5.57\text{E}(-4)$	$6.47\text{E}(-3) \pm 1.62\text{E}(-3)$	$6.92\text{E}(-3) \pm 1.08\text{E}(-3)$
90	$4.26\text{E}(-3) \pm 4.69\text{E}(-4)$	$7.52\text{E}(-3) \pm 1.43\text{E}(-3)$	$1.02\text{E}(-2) \pm 2.04\text{E}(-3)$
95	—	—	$1.55\text{E}(-2) \pm 2.47\text{E}(-3)$
100	$4.65\text{E}(-3) \pm 7.01\text{E}(-4)$	$1.45\text{E}(-2) \pm 1.45\text{E}(-3)$	$2.02\text{E}(-2) \pm 2.83\text{E}(-3)$
105	$5.43\text{E}(-3) \pm 7.12\text{E}(-4)$	$1.63\text{E}(-2) \pm 1.47\text{E}(-3)$	$2.34\text{E}(-2) \pm 2.81\text{E}(-3)$
110	$4.22\text{E}(-3) \pm 6.21\text{E}(-4)$	$1.78\text{E}(-2) \pm 1.42\text{E}(-3)$	$2.45\text{E}(-2) \pm 2.93\text{E}(-3)$
115	$4.62\text{E}(-3) \pm 6.10\text{E}(-4)$	$1.52\text{E}(-2) \pm 1.06\text{E}(-3)$	$2.45\text{E}(-2) \pm 2.94\text{E}(-3)$
120	$4.00\text{E}(-3) \pm 6.01\text{E}(-4)$	$1.42\text{E}(-2) \pm 9.95\text{E}(-4)$	$1.96\text{E}(-2) \pm 2.67\text{E}(-3)$
125	$2.73\text{E}(-3) \pm 4.051\text{E}(-4)$	$9.56\text{E}(-3) \pm 1.00\text{E}(-3)$	$1.69\text{E}(-2) \pm 2.03\text{E}(-3)$
130	$2.28\text{E}(-3) \pm 3.63\text{E}(-4)$	$6.56\text{E}(-3) \pm 8.00\text{E}(-4)$	$9.59\text{E}(-3) \pm 1.15\text{E}(-3)$

Equation (21) can be used to generate differential cross sections for small values of  $K^2$  based on the first Born approximation. These are shown in figure 8. It is clear that the present results agree very well with these generated cross sections for angles less than  $10^\circ$ . At scattering angles greater than this the assumption of the weakness of the interaction breaks down and the computed values exceed the measured values.

Differential cross sections at small angles for an incident energy of 60 eV are shown in figure 9. They are compared with the predictions of Pangantiwar and Srivastava (1988). As was the case at 20 eV these theories overestimate the cross sections at small angles but in this case the fair agreement between the DWPE calculation and the present results is extended out to about  $20^\circ$ . The results of the close-coupling calculation of Msezane and Henry (1986b) are also shown. The agreement in shape between the present results

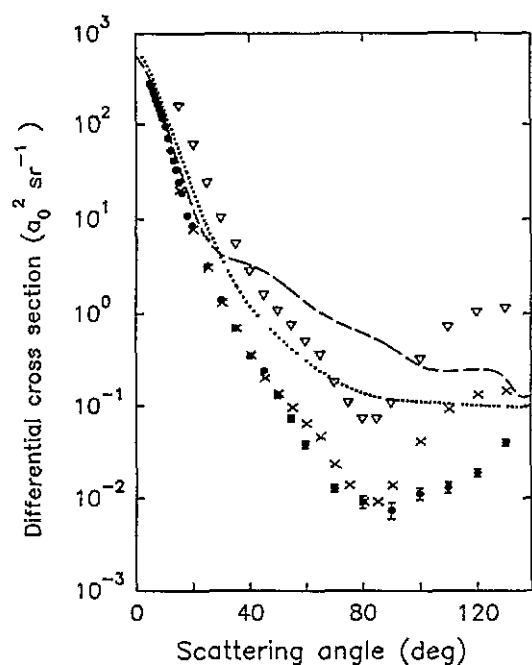


Figure 7. Differential cross sections for the excitation of the  $3d^{10}4p^2P$  state in copper at an incident energy of 20 eV. The present results ( $\bullet$ ) are compared with those of Trajmar *et al* (1977) ( $\nabla$ ) and with a renormalized version ( $\times$ ). The predictions of Srivastava *et al* (1988) are shown as (.....) distorted-wave exchange (DWE) and (— — —) distorted wave with polarization potential (DWPE).

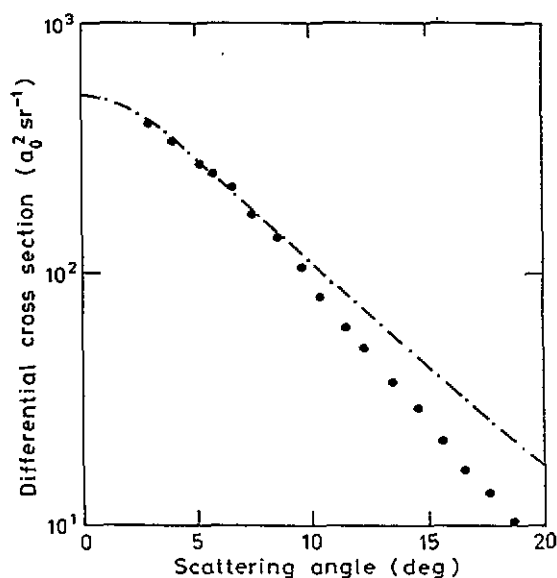


Figure 8. The present differential cross sections ( $\bullet$ ) compared with cross sections generated from (21) at 20 eV.

and this theory is very good but there is a significant difference in the absolute value of a factor of about 2.8. This difference is puzzling given the excellent agreement between the total cross sections derived from the present results and those reported by Msezane and Henry (1986a) using the same theory. Indeed if the integral cross section is calculated from the close-coupling results shown in figure 9 it is found that this value differs from the published value by a factor of about 2.8. It is tempting to propose that the disagreement between the present results and the close-coupling theory arises from a numerical error that has been made in the reported differential cross sections of Msezane and Henry.

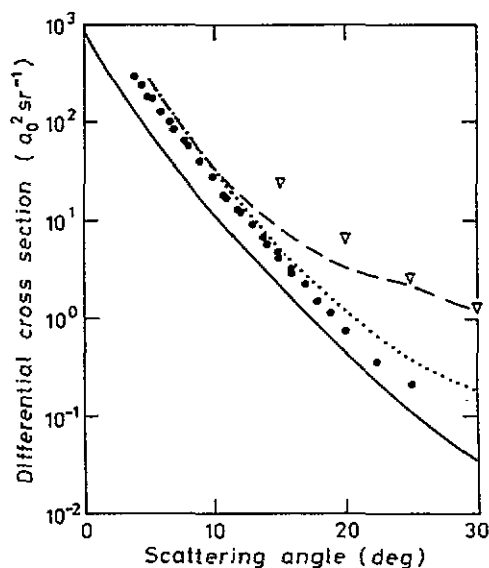


Figure 9. Small angle differential cross sections for the excitation of the  $^2P$  state at 60 eV. The present results ( $\bullet$ ) are compared with the DWE (.....) and DWPE (---) calculations of Pangantiwar and Srivastava (1988). The predictions of the close-coupling calculation of Msezane and Henry (1986b) are shown (—). The data of Trajmar *et al* (1977) are shown as ( $\nabla$ ).

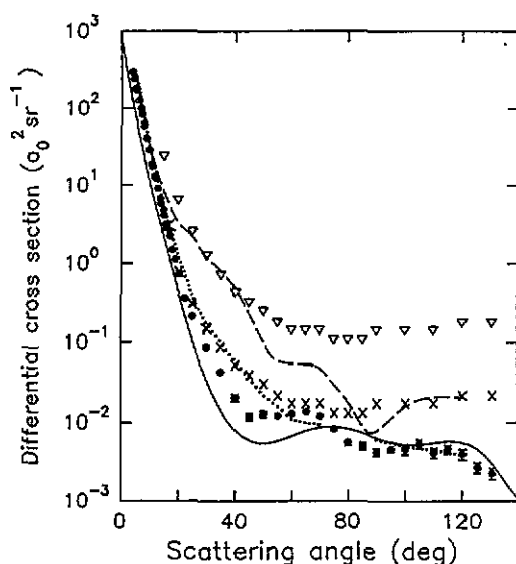
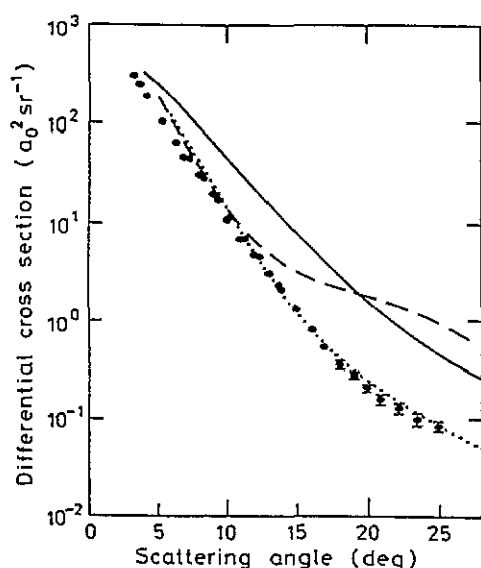
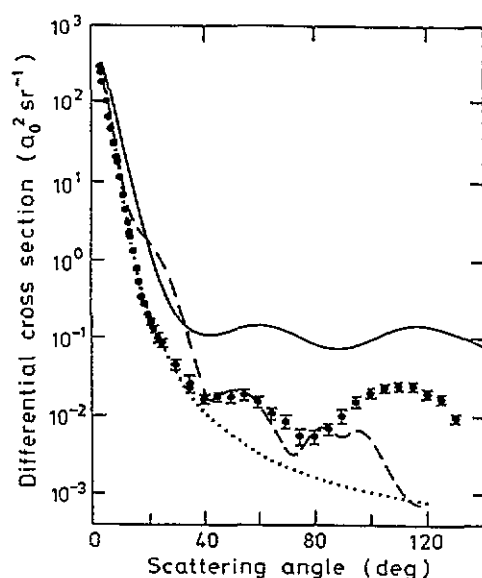


Figure 10. Differential cross sections for the excitation of the  $^2P$  state at 60 eV over the whole angular range. The legend is as for figure 9 except a renormalized set of the results of Trajmar *et al* (1977) shown as ( $\times$ ).

The cross sections at 60 eV over the whole angular range are shown in figure 10. In this case the distorted-wave exchange calculation and the distorted-wave polarization calculation of Pangantiwar and Srivastava fail to predict the first minimum at about  $50^\circ$ . The close-coupling calculation predicts this minimum and apart from the problem with the absolute value described above shows good agreement out to about  $60^\circ$ . The previous measurements of Trajmar *et al* (1977) are about a factor of ten larger than the present results at middle angles. This is significantly greater than that implied by the suggested renormalizing factor of 0.36 of Msezane and Henry (1986). It is noted that Msezane and Henry (1986b) showed better agreement between their theory and the 'renormalized' results of Trajmar *et al* (1977) than is implied in figure 10. This appears to have been achieved by reducing the previous experimental data by a factor of about 12 over a



**Figure 11.** Small angle differential cross sections for the excitation of the  $2P$  state at 100 eV. The present results ( $\bullet$ ) are compared with the DWE (.....) and DWPE (---) calculations of Pangantiwar and Srivastava (1988). The predictions of the close-coupling calculation of Msezane and Henry (1986b) are shown (—).



**Figure 12.** Differential cross sections for the excitation of the  $2P$  state at 100 eV over the whole angular range. The legend is as for figure 11.

large angular range. The paper by Pangantiwar and Srivastava (1988) indicates that these renormalized data are now established in the literature. Given the ambiguities associated with the published differential cross sections from the close-coupling theory the use of renormalized results based on this theory is misleading. As we did at 20 eV we show our renormalized results of Trajmar *et al* (1977). In this case these data have been produced by multiplying the published results by the constant factor of 0.13 which was determined from the normalizing procedure used at 20 eV. The good agreement at forward angles between the two sets of measurements demonstrates that the technique used by Trajmar *et al* to determine the energy dependance of their differential cross sections was valid.

The present results at 100 eV are shown in figure 11 for scattering angles less than  $30^\circ$ . The close-coupling results are in serious disagreement with the present measurements. As was the case at 60 eV we are unable to reproduce the published integral cross sections of Msezane and Henry (1986a) with the differential cross sections given in the paper by Msezane and Henry (1986b). In this case the problem is more serious than a possible simple numerical factor because the shapes are very different.

The predictions of the DWE theory show better agreement with the present results at this energy than they did at 60 eV. However, these results are too large at small angles which is consistent with the disagreement with the observations of the total cross section. The influence of the polarization potential as shown by the DWPE calculation by Pangantiwar and Srivastava (1988) makes matters worse. This calculation does introduce structure in the predicted results which is observed in the present measurements at  $40^\circ$  and around  $80^\circ$  as shown in figure 12. The close-coupling theory predicts minima in the cross section at

around these angles but the magnitude of the predicted cross sections are a factor of about 10 too high at middle angles.

#### 4. Conclusions

The origin of the experiments reported in this paper was stimulated by the proposal of Msezane and Henry (1986b) that further experiments were required on the scattering of electrons from copper so that the disagreement between theory and the earlier experiments of Trajmar *et al* could be resolved. Msezane and Henry attributed the disagreement to a problem with the normalization of the experiments and observed that the experiments were very difficult to perform. We agree with this latter observation and our results show that their assertion about the normalization problem is substantially correct. Msezane and Henry focused on the difficulties associated with the experiments but it is true that the theoretical problem is also very difficult. An adequate description of the bound states in the copper atom is essential before the various approximations are applied. The success of the Msezane and Henry calculation in predicting the total cross section demonstrates the validity of the wavefunctions which they used rather than the success of the close-coupling theory. If it was not for the ambiguities discovered with the close-coupling differential cross sections, it could be argued that there is no need for further calculations using the close-coupling approximation at these energies. However, the close-coupling predictions do not agree with the present differential cross sections for inelastic scattering and they are inconsistent with the published total cross sections. Therefore it is clear that further theoretical effort needs to be devoted to this difficult problem.

In the context of the copper vapour laser problem where energies less than 20 eV are important, the disagreement between the present integral cross section and the close-coupling results of Msezane and Henry at 20 eV also indicates the need for additional theory.

The present results imply that a Born approximation calculation for the excitation of the  $3d^{10}4p\ ^2P$  state at energies in excess of 60 eV should give adequate results for the total cross section provided appropriate wavefunctions are used. To first order the suitability of the wavefunction can be tested by the optical oscillator strength which is well established. Such calculations, when extended to other states, are useful in estimating the contribution of cascades to the population of the upper and lower states in the copper vapour laser.

#### Acknowledgments

The assistance of Mr R Houghton and Dr G F Shen during early phases of this work is gratefully acknowledged as is the dedication and skill of Mr B Gilbert for the construction and modification of the copper oven. This work was supported in part by grants from the Australian Research Council.

#### References

- Aleksakhin I S, Borooik A A, Starodub V P and Shafranjosh I I 1979 *Zh. Prik. Spektrosk.* **30** 236
- Borozdin V S, Smimov Yu M and Sharonov Yu D 1977 *Opt. Spectrosc.* **43** 384
- Brunger M J, Riley J L, Scholten R E and Teubner P J O 1988 *J. Phys. B: At. Mol. Opt. Phys.* **21** 1639
- Flynn C, Wei Z and Stumpf B 1993 *Phys. Rev. A* **48** 1239
- Hannaford P and MacDonald D C 1978 *J. Phys. B: At. Mol. Phys.* **11** 1177
- Mott N F and Massey H S W 1965 *Theory of Atomic Collisions* 3rd edn (London: Oxford University Press)

- Msezane A Z and Henry R J W 1985 *Phys. Rev. Lett.* **55** 2277  
———1986a *Phys. Rev. A* **33** 1631  
———1986b *Phys. Rev. A* **33** 1636  
Pangantiwar A W and Srivastava R 1988 *J. Phys. B: At. Mol. Phys.* **21** 2655  
Peterkop R and Liepinsh A 1979 *Latv. PSR Zinat Vestis Fiz. Teh. Zinat.* **2** 3  
Schiebner K F, Hazi A V and Henry R J W 1987 *Phys. Rev. A* **35** 4869  
Teubner P J O, Riley J L, Brunger M J and Buckman S J 1986 *J. Phys. B: At. Mol. Phys.* **19** 3313  
Trainor D, Mandl A and Hyman H 1975 cited in Msezane and Henry 1985 (unpublished)  
Trajmar S, Williams W and Srivastava S K 1977 *J. Phys. B: At. Mol. Phys.* **10** 3323  
Williams W and Trajmar S 1974 *Phys. Rev. Lett.* **33**, 187  
Winter N W 1977 cited in Trajmar *et al* 1977 (unpublished)  
Winter N W and Hazi A V 1982 cited in Msezane and Henry (1986a) (unpublished)